

## Neutral hydrogen in IC 342 – I. The large-scale structure

K. Newton *Mullard Radio Astronomy Observatory, Cavendish Laboratory,  
Madingley Road, Cambridge CB3 0HE*

Received 1979 September 11

**Summary.** An aperture synthesis survey of H I in the Scd galaxy IC 342 is described, with radial velocity resolution  $16 \text{ km s}^{-1}$  and a maximum angular resolution of  $1.9 \times 2.0$  arcmin. There is large-scale asymmetry, with a low-brightness extension to the north-west reaching 52 kpc from the nucleus. The velocity field shows deviations from normal rotation in the outer parts of the galaxy which are interpreted as warping of the galactic plane. The data are consistent with a flat rotation curve out to at least 42 kpc. If the rotation curve is flat at greater radii, the ‘north-west extension’ is also warped, but not so strongly as expected from an extrapolation of the perturbations observed at smaller radii. A tidal interaction is an attractive explanation for the disturbances.

### 1 Introduction

IC 342 is an Scd galaxy of luminosity class ScI, which has well developed spiral structure and is almost face-on. It is one of the largest galaxies in the northern sky, but its proximity to the Galactic plane ( $b = 10.6^\circ$ ) results in high obscuration and there are few optical data other than a photometric study by Ables (1971). The low systemic velocity means that H I observations are confused by emission from local Galactic hydrogen. Single-dish studies (Dieter 1962; Davies 1974) are particularly difficult due to the characteristic large-scale of the local H I, but aperture synthesis measurements are probably more reliable and such observations were presented by Rogstad, Shostak & Rots (1973) with an angular resolution of 4 arcmin, although they did not cover the aperture plane fully.

Neutral hydrogen has been detected to much larger distances from the nucleus than either optical or radio continuum emission, but little is known about the dynamics of the gas at large radii. Further synthesis measurements with good sensitivity and high spatial and spectral resolution are therefore important, particularly in view of recent studies of the radio continuum (e.g. Baker *et al.* 1977 and references therein). This paper presents a new aperture synthesis survey of IC 342; details of the observations and data reduction are described and the large-scale structure of IC 342 is discussed. High-resolution maps will be presented in a subsequent paper (Paper II) which deals with the spiral structure and kinematics.

Recent estimates of the distance to IC 342 cover a wide range of values but now appear to be converging. A detailed comparison with the very similar galaxies M101 and NGC 6946 (Newton 1978) yields a distance of 5 Mpc. Tammann (communicated to Baker *et al.* 1977) has derived a new value of  $4 \pm 1$  Mpc and for this discussion a distance of 4.5 Mpc will be adopted, in line with Rogstad *et al.* (1973) and Baker *et al.* (1977); this gives a scale factor of  $1 \text{ arcmin} \equiv 1.31 \text{ kpc}$ .

## 2 Observations and data reduction

### 2.1 OBSERVATIONS

Table 1 gives details of a survey made with the Cambridge Half-Mile telescope centred on the nucleus of IC 342. Complete coverage of the aperture plane was achieved by 12-hr observations at 48 interferometer baselines from 12.2 to 298.7 m at intervals of 6.1 m, giving maps

**Table 1.** Details of the observations.

Map centre (1950.0)	
RA	$03^{\text{h}} 41^{\text{m}} 58^{\text{s}}$
Dec	$67^{\circ} 56' 27''$
Mean epoch of survey	1975.2
FWHP of primary beam	94 arcmin
Observed range of radial velocities	+209 to -200 km/s
Angular resolution	
12-spacing observations	$7.0 \times 7.6 \text{ arcmin}$
24-spacing observations	$3.6 \times 3.9 \text{ arcmin}$
48-spacing observations	$1.9 \times 2.0 \text{ arcmin}$
Observed rms noise over single output map	
12-spacing observations	0.13 K
24-spacing observations	0.36 K
48-spacing observations	1.20 K

with a maximum resolution of  $1.9 \times 2.0 \text{ arcmin}$ . Maps were also made, using the 12 smallest baselines, with a resolution of  $7.0 \times 7.6 \text{ arcmin}$  for investigation of large-scale structure; maps with an intermediate resolution were useful for some purposes.

A 160-channel digital cross-correlation spectrometer was used to measure H I emission over a 2-MHz ( $\equiv 422 \text{ km s}^{-1}$ ) bandwidth centred on 1420.4 MHz. The output spectrum, with a resolution of  $16 \text{ km s}^{-1}$ , provided 32 output maps at velocity intervals of  $13.2 \text{ km s}^{-1}$ . Broadband emission over a 10 MHz bandwidth centred on 1419.0 MHz was measured simultaneously. The survey was calibrated using 3C 309.1 which was assumed to be unpolarized with a flux density of 7.9 Jy. In order to correct for the presence of continuum emission, the output maps which contained no significant H I emission were averaged and subtracted from those which did.

The absence of interferometer spacings smaller than the diameter of the paraboloids (i.e.  $\leq 45 \lambda$ ) means that (i) no structure on a scale larger than  $\sim 1^{\circ}$  can be detected and (ii) a variation in zero-level is introduced across the output maps. After applying a simple first-order correction for the latter (Newton 1978), residual effects are typically 5 per cent of the

peak amplitudes on output maps not contaminated by local H I, a value comparable with sidelobe effects. The instrumental noise on the low-resolution maps (Table 1) is generally less than this where emission is detected, so, on those maps not contaminated by local H I, extended emission brighter than 1 K is taken as being from IC 342. The effect of residual zero-level variation was minimized by setting to zero the values at all grid-points outside the region of detected emission from IC 342 on each output map before further analysis. In addition, the average local zero-level around emission from IC 342 was determined and each map adjusted accordingly. Considerable variation in zero-level remains on the three maps most confused by local H I, but the effect was again reduced by the correction for local H I described in Section 2.2. Velocity profiles were constructed from the resulting maps of line emission and analysed in the usual way (Warner, Wright & Baldwin 1973; Winter 1975a) to produce maps of integrated hydrogen and velocity dispersion. Only those points in the profiles having contributions greater than 1.5 times the mean rms noise level were included in the integration. Maps of radial velocity were obtained by making a least-squares fit of a Gaussian to each profile, and assigning to it the velocity of the peak of the Gaussian.

All map coordinates are for epoch 1950.0 and radial velocities are heliocentric.

## 2.2 CORRECTION FOR LOCAL HYDROGEN

The proximity of IC 342 to the Galactic plane indicates that 21-cm emission from local H I would be expected on those output maps close to  $0 \text{ km s}^{-1}$ . Inspection of the output maps (Fig. 1) shows such emission to be present over the radial velocity range from  $-2$  to  $-68 \text{ km s}^{-1}$ . The two major effects of this local H I are confusion and absorption.

### 2.2.1 Confusion

The large angular scale characteristic of local H I, together with the fact that the Half-Mile telescope is not sensitive to emission on a scale greater than  $\sim 1^\circ$ , means that confusion will be relatively unimportant and certainly less than in single-dish observations. In order to investigate the distribution of H I in IC 342, maps of integrated hydrogen and radial velocity were produced by excluding, in the contaminated range of velocities ( $-2$  to  $-68 \text{ km s}^{-1}$ ), emission outside the rectangles shown in Fig. 1. Such emission typically has the following characteristics:

- (a) low brightness, with low values of velocity dispersion;
- (b) no continuity, either spatially or in radial velocity, with the emission closer to the nucleus of IC 342;
- (c) neither the radial velocity nor spatial distribution expected for IC 342 by comparison with the north-east (uncontaminated) half of the galaxy.

It is therefore likely to be local Galactic hydrogen. The procedure will have *excluded* some H I belonging to IC 342 and *included* some low-brightness local H I, but this will have little effect on the following discussion.

### 2.2.2 Absorption

Although much of the large-scale local H I is not visible as emission in the present survey, it does absorb radiation from IC 342 and this effect is most significant on the  $-15 \text{ km s}^{-1}$  output map. The absorption was estimated from (i) spectral profiles of 4C 67.08 and

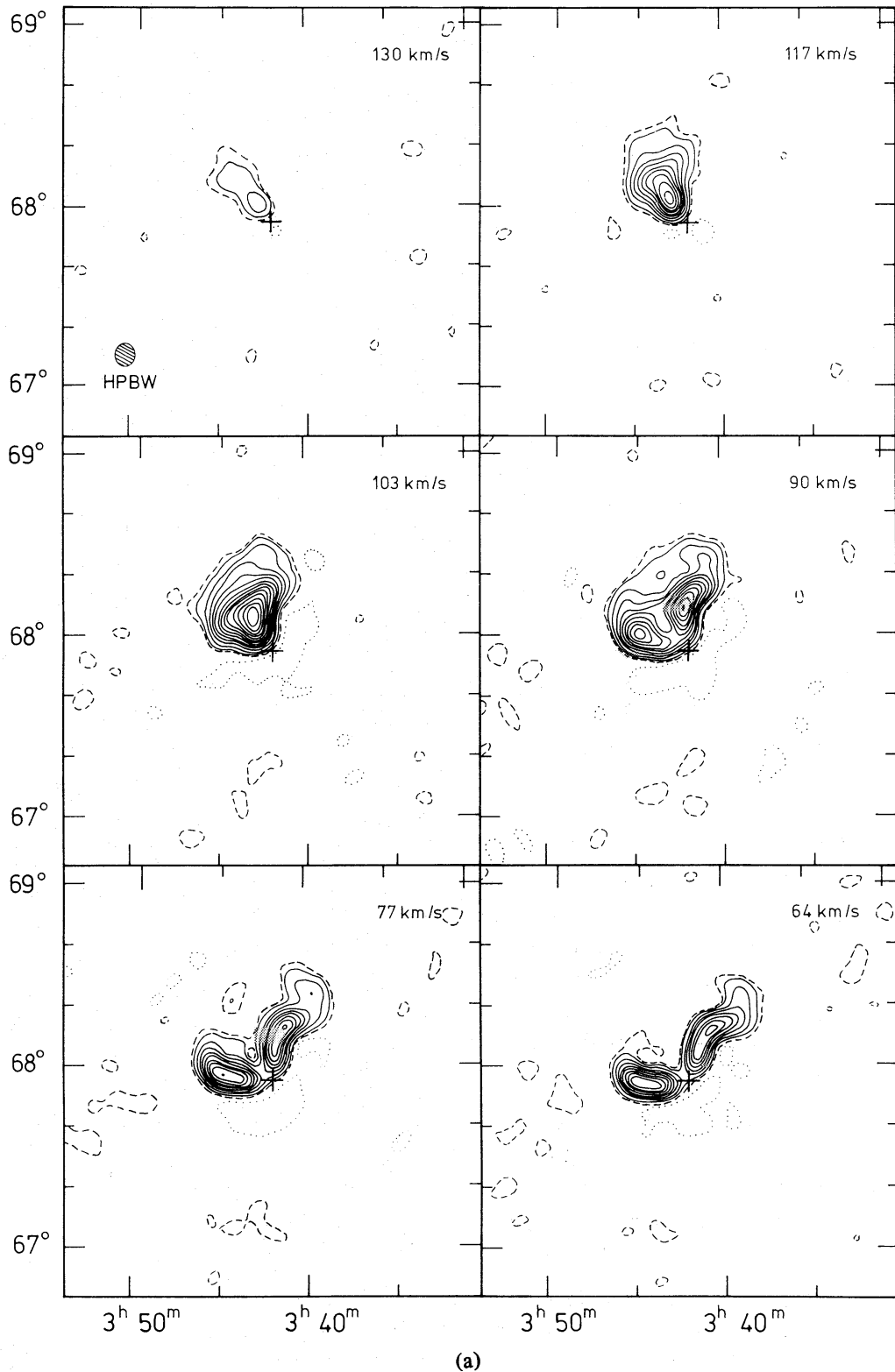


**Figure 1.** IC 342: The output maps at  $7.0 \times 7.6$  arcmin resolution with contour intervals 1 K at the map centres; the first negative contour is dotted and, where shown, the dashed contour is at 0.5 K. The nucleus is indicated by a cross. See text for explanation of the rectangles drawn on Fig. 1(b) and (c). None of these maps or the following maps of integrated HI are corrected for the primary beam response, so the rms noise is uniform across each map. This response approximates well to a Gaussian of FWHP 94 arcmin.

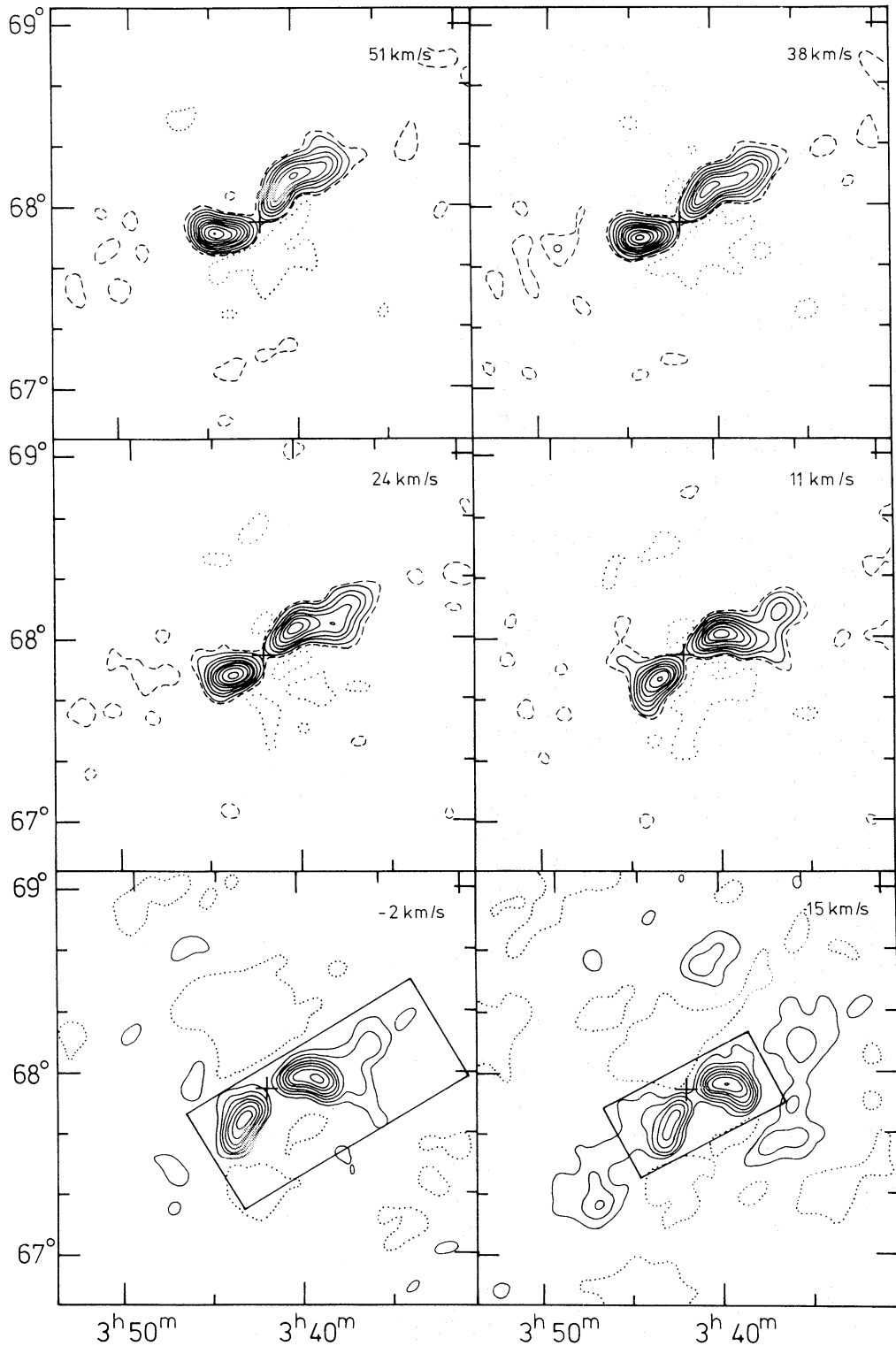


Fig. 1(b)

4C 67.09 (30 and 32 arcmin from the nucleus of IC 342 respectively) at  $1.9 \times 2.0$  arcmin resolution, and (ii) the brightness temperature of Galactic HI emission (Fig. 2), assuming a spin temperature of 120 K. The two estimates are consistent, and upwards corrections of 15, 30 and 15 per cent were applied to the  $-2$ ,  $-15$  and  $-29$   $\text{km s}^{-1}$  maps as observed.

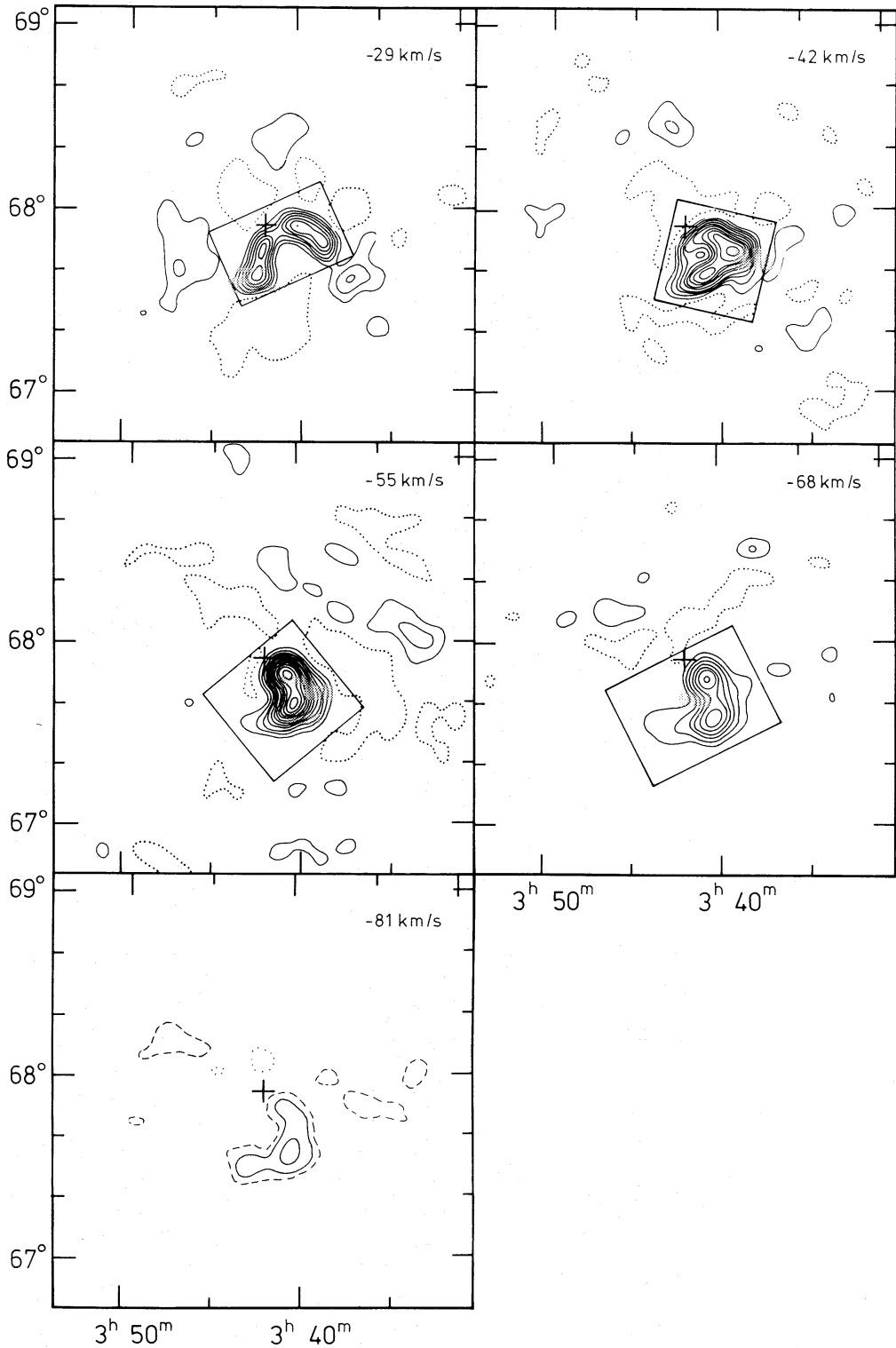


Fig. 1(c)

### 2.2.3 Comparison with single-dish observations

The solid line in Fig. 2 is a profile taken from the Berkeley survey (Heiles & Habing 1974) at the position of the nucleus of IC 342 and convolved to a radial-velocity resolution of  $16 \text{ km s}^{-1}$ . Although emission extends from  $+20$  to  $-60 \text{ km s}^{-1}$ , the peak at  $-12 \text{ km s}^{-1}$

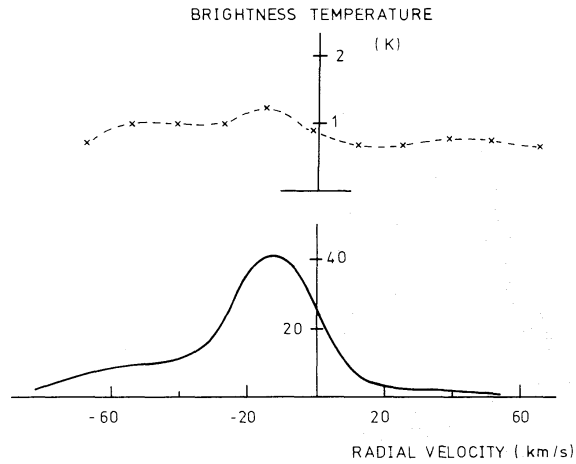


Figure 2. 21-cm profiles at the map centre of the IC 342 survey derived as described in the text: solid line – Berkeley single-dish survey (Heiles & Habing 1974); broken line – present survey.

contributes mainly to one output map, that at  $-15 \text{ km s}^{-1}$ . The broken line in Fig. 2 indicates the average brightness temperatures observed within  $0.6^\circ$  (the Berkeley HPBW) of the map centre in the present survey at  $7.0 \times 7.6$  arcmin resolution, measured from the maps shown in Fig. 1. The difference between the curves indicates that only a small fraction of the local H I is seen in emission by the present survey, due to the insensitivity of the Half-Mile telescope to emission on a scale  $\geq 1^\circ$ .

### 3 The large-scale H I distribution

Fig. 3 shows the  $7.0 \times 7.6$  arcmin resolution map, integrated over a range in radial velocity of  $-81.2$  to  $+129.8 \text{ km s}^{-1}$  and excluding local Galactic hydrogen. The outer (broken) contour is taken from the individual output maps and indicates the limit of detected H I associated

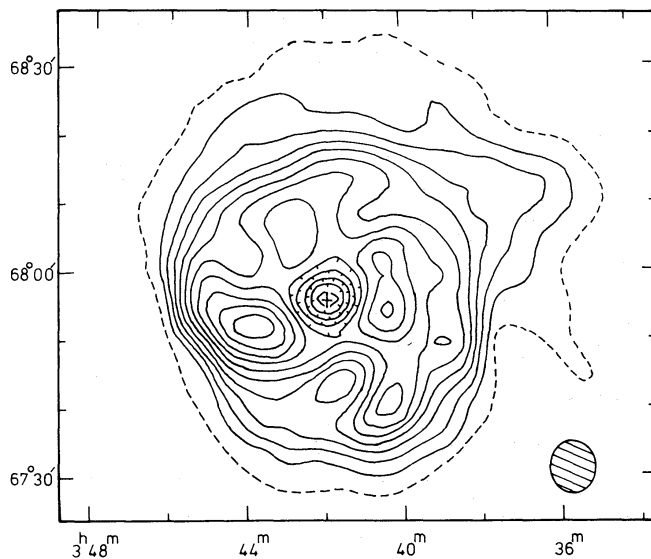
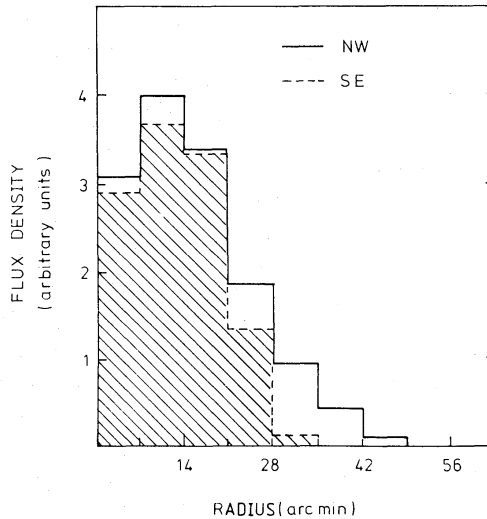


Figure 3. IC 342: The integrated hydrogen map at  $7.0 \times 7.6$  arcmin resolution, uncorrected for the primary beam response. The contour interval at the map centre is  $50 \text{ K km s}^{-1}$  and the first solid contour is at  $75 \text{ K km s}^{-1}$ . The outer (broken) contour is taken from the output maps and shows the extent of detected H I associated with IC 342.

with IC 342. With the exception of the north-west quadrant, the H I extent is roughly elliptical and reaches 25–35 arcmin from the nucleus. In the central area there is good agreement with the observations by Rogstad *et al.* (1973). Around the outermost edge of the H I, again with the exception of the north-west extension, there is a steep gradient in the emission which is most apparent to the east.

The central depression in H I emission is unresolved by the  $7.0 \times 7.6$  arcmin beam, and has a half-power diameter of  $\approx 9$  kpc. Investigation of the high-resolution maps gives an upper limit to the column density in this region of  $2.7 \times 10^{20}$  atom  $\text{cm}^{-2}$ , showing the depletion to be real and not simply due to the large range of velocities present near the nucleus. Davies (1974) noted an extension of low brightness H I emission to the north-west of IC 342. In the north-west quadrant of Fig. 3, H I is detected to a distance of 43 arcmin (52 kpc) from the nucleus in the plane of the sky at a level  $\approx 1.5 \times 10^{20}$  atom  $\text{cm}^{-2}$ . This extends considerably further than emission detected by Rogstad *et al.* in the previous synthesis survey, where H I emission was found in the north-west out to 30 arcmin. The north-west extension has a relatively low surface brightness ( $\sim 150$  K  $\text{km s}^{-1}$ ) and the emission tails off gradually.



**Figure 4.** Radial distribution of H I flux density, averaged in semi-circular rings in the plane of IC 342 (assuming major axis p.a. =  $39^\circ$ , inclination =  $25^\circ$ ) on each side of the major axis.

The asymmetry of the outer region is clearly indicated by Fig. 4, which shows the H I flux density averaged in semi-circular rings in the plane of the galaxy. Within  $R = 20$  arcmin, the *averaged* H I emission is quite symmetrically distributed between the two halves of the galaxy, although there is a massive feature about 15 arcmin east of the nucleus (Fig. 3) with peak integrated brightness temperatures of  $525$  K  $\text{km s}^{-1}$ .

The relation between H I and optical emission is shown in Plate 1. Neutral hydrogen extends to much greater radii than the optical emission, which Ables (1971) detected only to a maximum radius of 20 arcmin for a limiting surface brightness of  $26.51$  mag  $\text{arcsec}^{-2}$ . Large-scale spiral structure is visible, even at the low resolution of Fig. 3, with features to the north, east and west following roughly the optical spiral pattern.

Fig. 5 shows the variation of total H I flux density in IC 342 as a function of radial velocity, obtained by spatial integration of the individual output maps. Profiles are shown for the surveys both at  $7.0 \times 7.6$  and  $1.9 \times 2.0$  arcmin resolution. The difference between the two curves gives an indication of the amount of low-brightness, large-scale structure missing



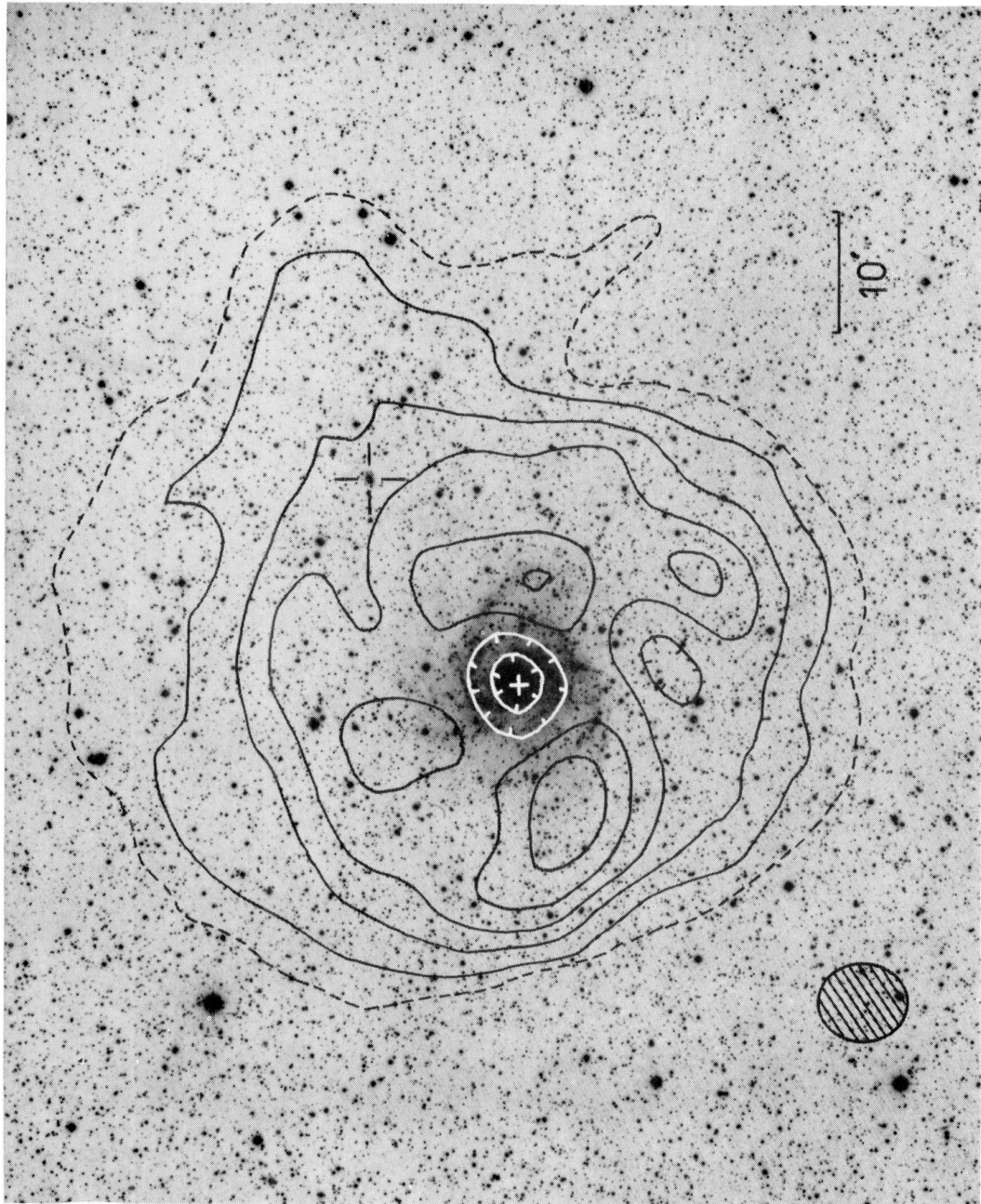


**Plate 1.** Contours from the  $7.0 \times 7.6$  arcmin resolution map of integrated H I (Fig. 3) superimposed on a 48-in. Schmidt photograph of IC342 taken in red light. (Photograph copyright by the National Geographic Society–Palomar Observatory Sky Survey. Reproduced by permission from the Hale Observatories.) The contour interval is  $100 \text{ K km s}^{-1}$  at the map centre; the first solid contour is at  $75 \text{ K km s}^{-1}$  and the broken line is taken from Fig. 3. The open cross marks the position of UGCG 2826 (see text). North is towards the left, and west towards the top of the plate.

[facing page 176]



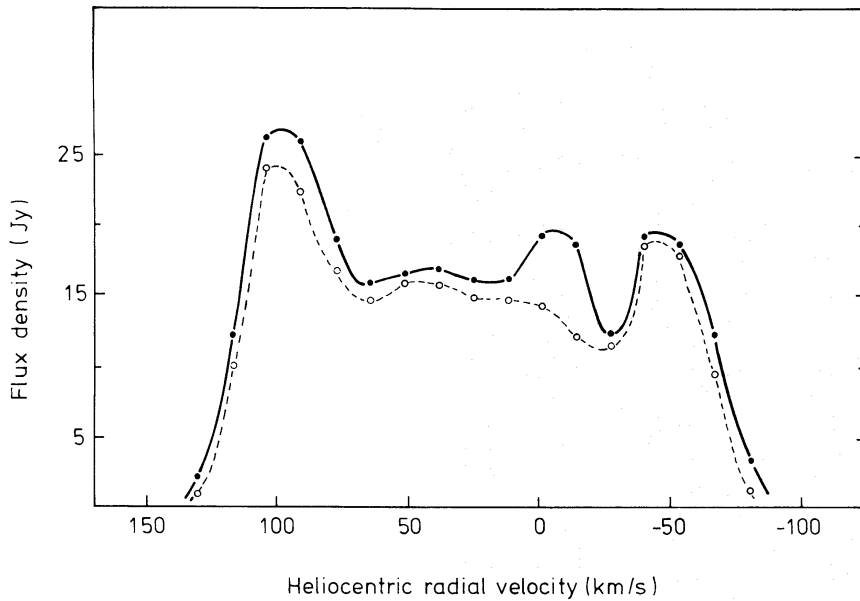


**Figure 5.** Integrated line profile for IC 342, corrected for absorption. Solid line: data at 7-arcmin resolution. Broken line: data at 1.9-arcmin resolution.

from the high-resolution maps (which will be discussed in Paper II). Fig. 5 is in reasonable agreement with the profile given by Rogstad *et al.* (1973). The total observed H I mass is  $1.7 \times 10^{10} M_{\odot}$ , compared with the value of  $1.5 \times 10^{10} M_{\odot}$  obtained by Rogstad *et al.* The mass of H I associated with the 'north-west extension' is  $2 \times 10^9 M_{\odot}$ .

## 4 The radial velocity field

### 4.1 OVERALL PROPERTIES

The radial velocity field at  $7.0 \times 7.6$  arcmin resolution, determined by the method described in Section 2.1, as shown in Fig. 6. It has (i) a smooth and continuous variation over the map,

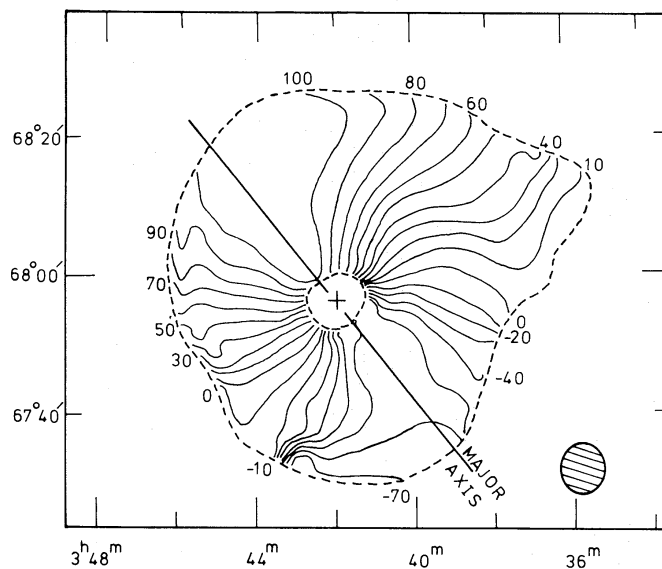


**Figure 6.** IC 342: The radial velocity field at  $7.0 \times 7.6$  arcmin resolution. The contour interval is  $10 \text{ km s}^{-1}$  and the rms noise is  $\approx 2 \text{ km s}^{-1}$ .

(ii) the form in the central regions ( $R < 16$  arcmin) expected for a galaxy in normal differential rotation, and (iii) deviations from 'normal' rotation in the outer regions, especially in the north-west extension.

#### 4.2 PARAMETERS OF THE CENTRAL DISC

The inclination, and p.a. of the major axis, were derived by subtracting model velocities (appropriate to a flat disc in various p.a.'s and inclinations, with the corresponding measured rotation curve) from the radial-velocity field of Fig. 6 and minimizing the residuals. This gave a value of  $39^\circ \pm 3^\circ$  for the p.a. of the major axis, and an inclination of  $25^\circ \pm 3^\circ$  for the central region ( $R < 16$  arcmin), together with a systemic velocity of  $+25 \pm 3$  km s $^{-1}$ , in good agreement with Rogstad *et al.* (1973) but not in accordance with the major-axis p.a. of  $97^\circ$  derived by Ables (1971) from the optical appearance.

Inspection of Fig. 6 shows that at greater radii the dynamical major axis, defined as the locus of maximum deviation from systemic velocity, bends towards the west in the north-east and towards the east in the south-west. This is a phenomenon seen in other nearby

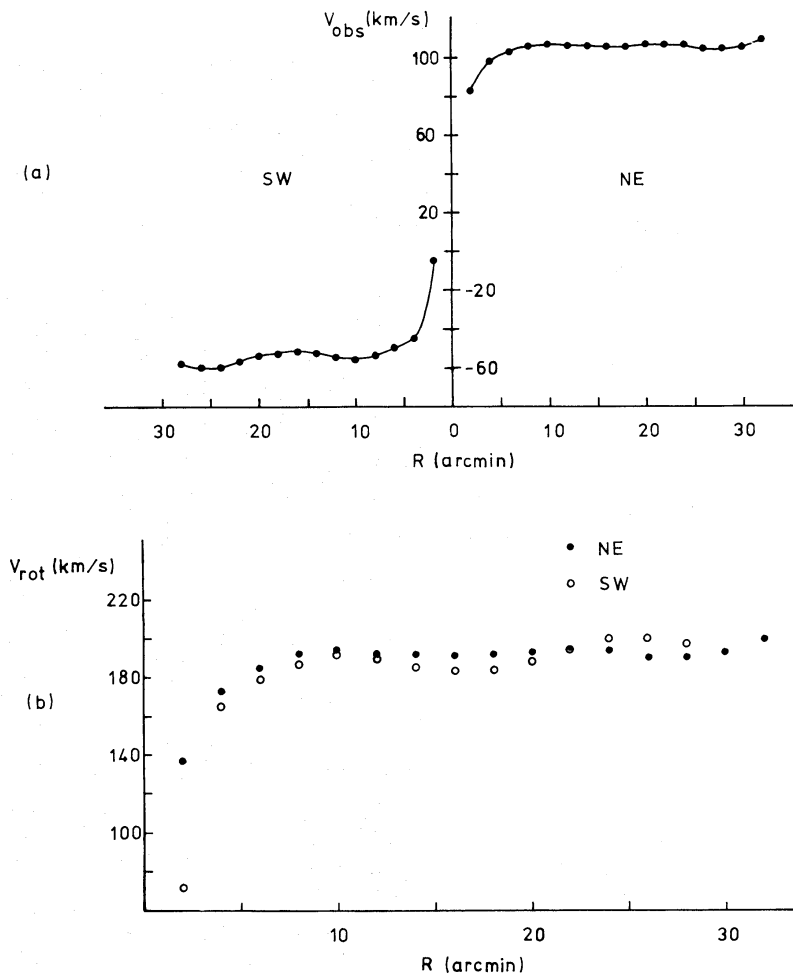


Figure 7. (a) Observed velocities,  $V_{\text{Obs}}$ , in IC 342 measured northwards and southwards along the major axis (p.a.  $39^\circ$ ). (b) Rotation curve (smoothed by the resolution of the synthesized beam along the major axis) derived from (a) above, assuming an inclination of  $25^\circ$  and  $V_{\text{sys}} = 25$  km s $^{-1}$ . The rms noise for  $V_{\text{Obs}}$  is  $\approx 2$  km s $^{-1}$ .

galaxies such as M83 (Rogstad, Lockhart & Wright 1974), M31 (Newton & Emerson 1977) and M33 (Reakes & Newton 1978).

In the central region ( $R < 16$  arcmin), measurements of the dynamical major axis yield a p.a. of  $39^\circ \pm 2^\circ$ , in good agreement with the value derived above by model-fitting to the whole velocity field in this area.

#### 4.3 THE ROTATION CURVE

Fig. 7(a) shows the variation of observed radial velocity along the major axis in p.a.  $39^\circ$ . On the assumption of a disc inclination of  $25^\circ$  and systemic velocity  $25 \text{ km s}^{-1}$ , the corresponding rotation velocities are shown in Fig. 7(b). This rotation curve, although smoothed by the  $7.0 \times 7.6$  arcmin beam, has a very steep central gradient and rapidly reaches a constant value, again in good agreement with Rogstad *et al.* for  $R < 19$  arcmin. At greater radii, these observations are consistent with a flat rotation curve; indeed the peak deviation of the mean (average of the north-east and south-west curves) from a constant  $V_{\text{rot}}$  of  $191 \text{ km s}^{-1}$  is only  $\pm 9 \text{ km s}^{-1}$  over the entire region  $6 < R < 32$  arcmin ( $8 < R < 42 \text{ kpc}$ ). The values of  $V_{\text{rot}}$  are highly dependent on the inclination assumed, since the disc is close to face-on, and a difference of  $\pm 10^\circ$  in assumed inclination corresponds to a difference of  $\pm 30 \text{ km s}^{-1}$  in the value of  $V_{\text{rot}} = 191 \text{ km s}^{-1}$ . However, even in the warp model described below, Fig. 7(b) is likely to be a good representation of the true (smoothed) rotation curve, since the maximum change in inclination is only  $2^\circ$  and the variation of major axis p.a. with radius minimises even this effect along the line in p.a.  $39^\circ$ . The symmetry of the velocity field, i.e. the agreement between observed major axis velocities on either side of the minor axis, strongly suggests that to within a few  $\text{km s}^{-1}$  the observed velocities indeed result from circular rotation.

Using the rotation curve of Fig. 7(b) and the thin-disc model described by Emerson (1976), the total mass of IC 342 for  $R < 32$  arcmin (42 kpc) was derived on the assumption that the mass density is zero beyond 42 kpc. The value of  $2.6 \times 10^{11} M_\odot$  is similar to the masses of M31 and the Galaxy, although for different radii.

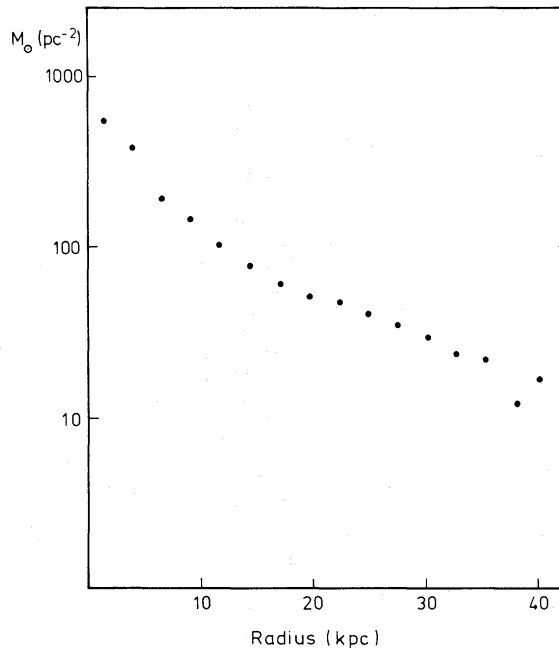


Figure 8. Radial variation of surface density of total mass.

Huchtmeier (1975) shows a rotation velocity of  $170 \pm 20 \text{ km s}^{-1}$  measured at  $R = 37$  arcmin (outside the detected limit of HI in the present survey); the same inclination of  $25^\circ$  was assumed and the measurement was made with the 100-m Effelsberg radio telescope. The indicated error of measurement does not allow us to determine whether this is significantly lower than the value of  $V_{\text{rot}} = 191 \text{ km s}^{-1}$  derived for smaller radii, but, in any case, a serious difficulty in the interpretation of isolated radial velocity measurements at large radii arises from the warping discussed below. Any low-brightness envelope of HI in the outer parts of the galaxy is likely to be warped, so observations of the large-scale velocity field of the gas are needed before an estimate of orbital parameters can be made. Nevertheless, Huchtmeier derived a value of  $6.2 \times 10^{11} M_\odot$  for the total mass, using the Brandt-curve method. Taking his measured velocity in conjunction with the present observations, and using the thin-disc model which makes no assumption about the behaviour of the rotation curve beyond those regions observed, a total mass of  $3 \times 10^{11} M_\odot$  for  $R < 37$  arcmin is obtained. The difference emphasizes the difficulty of extrapolating estimates of total mass to greater radii with any certainty. The only *objective* values are lower limits; until more sensitive observations allow the velocity field to be mapped at greater radii, the most stringent lower limit for the total mass of IC 342 is that of  $2.6 \times 10^{11} M_\odot$  (for  $R < 42 \text{ kpc}$ ) derived above. The variation of surface mass density with radius, projected perpendicular to the plane and calculated for the thin-disc model, is shown in Fig. 8.

#### 4.4 RADIAL VELOCITY PERTURBATIONS

The magnitude of perturbations from normal rotation can be seen from the residual-velocity map in Fig. 9, which displays the difference between observed and model radial velocities. The model consists of a thin flat disc with major axis p.a.  $39^\circ$ , inclination  $25^\circ$  and with the observed rotation curve for  $R < 16$  arcmin and a constant  $V_{\text{rot}} = 191 \text{ km s}^{-1}$  at greater radii.

Deviations at the southern edge of the HI envelope reach  $30 \text{ km s}^{-1}$  and would correspond to rotation velocities higher than the assumed flat rotation curve if the gas were confined to a flat disc. Similarly, the whole of the north-west extension is apparently rotating faster than the central region, with residuals of up to  $20 \text{ km s}^{-1}$ . In the north-west

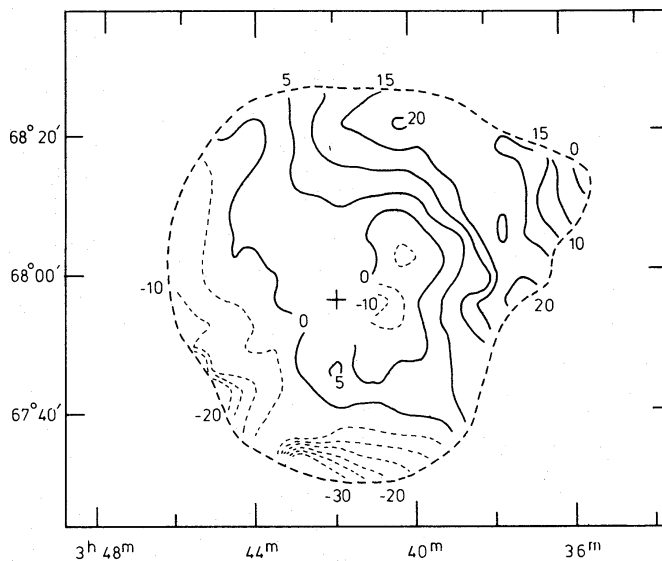


Figure 9. IC 342: Residual velocity field, showing the result of subtracting the velocities calculated for a flat-disc model from the observed radial-velocity field.

the magnitude of the perturbations increases from  $R = 12$  to 30 arcmin, but decreases thereafter. The distortions of the velocity field at the ends of the major axis in Fig. 5 are similar to those observed in several other galaxies, e.g. M83 (Rogstad *et al.* 1974) and M33 (Reakes & Newton 1978). In these cases the perturbations have been interpreted as evidence for warping of the galactic plane. In view of (i) the large physical scale of the perturbations in IC 342, (ii) the bending of the dynamical major axis, and (iii) the similarity of the radial-velocity field to those of other, warped, galaxies, the same explanation seems likely for IC 342.

#### 4.5 GEOMETRY

In the case of edge-on galaxies, the large-scale effects of warping on the H I distribution may be observed directly as distortions of the outer envelopes (e.g. Sancisi 1976). IC 342 is,

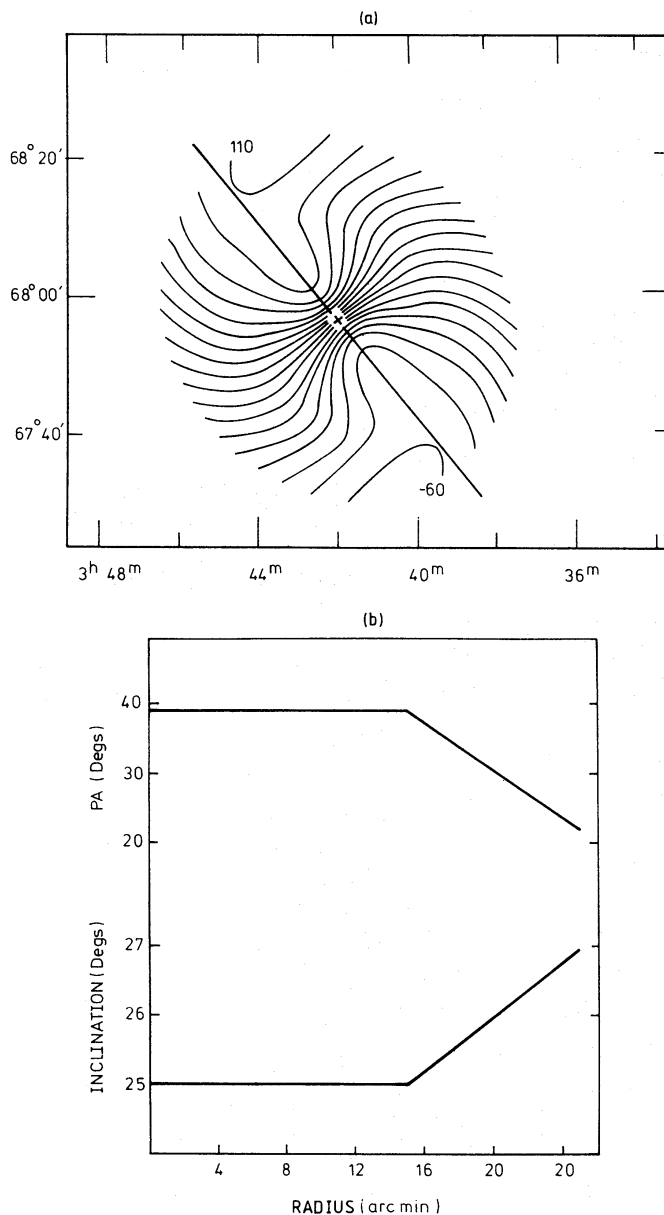


Figure 10. (a) Radial-velocity field corresponding to the warped-disc model for IC 342 described in the text. (b) The parameters of the warped disc model. Inclinations and p.a.'s of the major axis are defined relative to the plane of the sky (i.e. p.a.  $0^\circ$  is north, and inclination  $90^\circ$  indicates an edge-on disc).

however, nearly face-on and there is no symmetrical distortion of the H I *shape* apparent. On the other hand, the low inclination aids interpretation of the radial velocity field in terms of the geometry and kinematics of the H I distribution. Inspection of Fig. 6 indicates that some of the velocity perturbations in IC 342 are similar to those produced by a gradual variation with radius of the major-axis p.a. and inclination of the disc (e.g. Newton 1978). Perturbations associated with the north-west extension are, however, not continuous with those at smaller radii, so we shall initially confine our attention to the velocity field within a radius of 28 arcmin.

The perturbations within this region are somewhat asymmetrical over the disc, but the general trend is similar for deviations in the north and south, and the model shown in Fig. 10 fits the overall velocity field well. The model, similar to that described by Rogstad *et al.* (1974) to fit observations of M83 and subsequently applied to several other galaxies, is a system of rings, each in circular rotation about the nucleus of IC 342 and with the rotation curve shown in Fig. 7(b). The variation with radius of inclination and p.a. of the major axis (in the plane of the sky) is shown in Fig. 10(b). In this model H I reaches a height of  $\approx 2$  kpc above the plane of the central disc at  $R = 30$  kpc.

Simple extrapolation of the model will not explain the velocity perturbations observed in the north-west extension. Beyond  $R \approx 30$  arcmin, these are seen to decrease with radius, and the isovelocity contours return towards the configuration of normal differential rotation exhibited by the central region of the galaxy. Therefore, although the north-west extension may be warped, the magnitude of the distribution is not that expected from an extrapolation of the warp at smaller radii, on the assumption that  $V_{\text{rot}}$  is constant. It should be noted that the distortion may be consistent with an extrapolation of the model, if  $V_{\text{rot}}$  decreases with radius at large distances from the nucleus in the north-west.

The model presented above gives a good indication of the magnitude of the distortion, and the relation between the warp and spiral structure will be discussed in Paper II.

## 5 Discussion

Many galaxies are now known to be warped in their outer parts and the origin of the distortions is not yet clear in all cases (e.g. van der Kruit & Allen 1978 and references therein), although a tidal explanation remains attractive for some.

It is of interest to note that M101, already known to resemble IC 342 closely in other ways, also has an asymmetric H I distribution within the optically visible part of the galaxy. High-sensitivity observations of H I in the outer regions by Huchtmeier & Witzel (1979) show kinematical disturbances, with an 'S'-shaped major axis, extending to  $R \approx 90$  kpc (assuming a distance of 7.2 Mpc). In this case there is a nearby companion (NGC 5474) at a projected distance of 92 kpc, and a tidal interaction is a possible explanation for the perturbations (e.g. Winter 1975b; Huchtmeier & Witzel 1979). The search for a companion close to IC 342 is handicapped by the high optical obscuration (the extinction in blue light was estimated as 2.2 mag by Ables 1971), so that a nearby galaxy of low surface brightness may appear faint and with a small angular size on photographic plates. Rots (1979) has, however, recently found a probable companion for IC 342 by detection of H I emission at  $\approx 93$  arcmin (122 kpc if both galaxies are at 4.5 Mpc) south-east of IC 342 and with a similar radial velocity. This galaxy (labelled A0355 by Rots) is outside the present survey area. Rots' H I data, together with optical photometry, indicated the galaxy to be a late-type system with total mass  $2.1 \pm 1.1 \times 10^{10} M_{\odot}$  (for a distance of 4.5 Mpc). The configuration is very similar to that of M101 and NGC 5474. The system is also reminiscent of the pair M31–M33, which are separated by  $\sim 180$  kpc and which may have interacted (e.g. Reakes &



Newton 1978). A tidal interaction is therefore a likely explanation for the observed distortion in IC 342. This conclusion is strengthened by recent calculations concerning the remarkable persistence of gaseous warps. Tubbs & Sanders (1979) have shown that, under certain conditions, warps may persist for  $10^{10}$  yr. For a reasonable relative velocity (the difference between their radial velocities is  $\sim 50$  km s $^{-1}$ ). A0355 and IC 342 could have undergone a close passage well within such a time scale.

There are several other faint galaxies visible on Palomar Sky Survey plates in the vicinity of IC 342 and, by virtue of its position, the most likely of these to be associated with IC 342 is UGCG 2826 (*Uppsala General Catalogue of Galaxies*, Nilson 1973). This object is marked by a cross on Plate 1 and is located in the centre of the north-west extension in the region of largest velocity perturbation. There is no measured redshift, and no H I associated with UGCG 2826 has been detected by the present survey; there is, however, a single contour at the  $3\sigma$  level on the  $1.9 \times 2.0$  arcmin resolution broadband map, centred on the galaxy. The galaxy is unclassified but if it were, for example, a dwarf elliptical such as M32, an H I detection would not be expected. If UGCG 2826 is indeed close to IC 342, it could be the origin of the local disturbances observed in the north-west extension.

## 6 Conclusions

The most significant results of the new aperture synthesis survey of IC 342, with regard to the large-scale structure of the galaxy, are summarized below. Additional details are given in Table 2.

**Table 2.** IC 342: summary of properties.

Position (1950.0)		
RA		03 <sup>h</sup> 41 <sup>m</sup> 58 <sup>s</sup>
Dec		67 <sup>o</sup> 56' 27"
Assumed distance		4.5 Mpc
Inclination	} central disc R < 16 arcmin	25 <sup>o</sup> +/- 3 <sup>o</sup>
Major axis p.a.		39 <sup>o</sup> +/- 2 <sup>o</sup>
Heliocentric systemic velocity		+25 +/- 3 km/s
Observed H I mass $M_h$ ( $10^{10} M_\odot$ )		1.7
Total mass within $R = 42$ kpc $M_t$ ( $10^{11} M_\odot$ )		2.6
$M_h/M_t$		0.07

1. The overall extent of H I detected in IC 342, with the exception of the north-west quadrant, is roughly elliptical, reaching 25–35 arcmin from the nucleus (32.5–45.5 kpc in the plane of the sky, assuming a distance of 4.5 Mpc).

2. There are asymmetries in the H I distribution, notably an area of low-brightness emission to the north-west of the nucleus extending to  $R = 43$  arcmin (52 kpc) at a level of  $\sim 1.5 \times 10^{20}$  atom cm $^{-2}$  and a massive spiral feature to the east at a radius of 15 arcmin.

3. In the central regions of the galaxy ( $R < 16$  arcmin), the radial velocity field is consistent with a well-behaved disc in differential circular rotation. The rotation curve along the major axis (smoothed by the  $7.0 \times 7.6$  arcmin beam) is flat from  $R = 6$  arcmin to the limit of detected emission.

4. In the outer parts, there are large-scale deviations from normal rotation. The dynamical major axis deviates to the west in the north-east and to the east in the south-west,

perturbations consistent with warping of the galactic plane. Assuming a flat rotation curve at large radii, the 'north-west extension' is also warped, but not so strongly as expected from a simple extrapolation of the warp at smaller radii.

### Acknowledgments

I am grateful to many members of the Radio Astronomy Group for assistance with the observations and data analysis. I particularly thank Mr P. J. Warner for invaluable advice and Drs J. E. Baldwin and J. R. Shakeshaft for helpful discussions and comments on the manuscript. Financial support from the Science Research Council and the Royal Commission for the Exhibition of 1851 is gratefully acknowledged.

### References

- Ables, H. D., 1971. *Publs U.S. Naval Obs. Sec. Ser.* Vol. xx, Part IV, Washington, D.C.
- Baker, J. R., Haslam, C. G. T., Jones, B. B. & Wielebinski, R., 1977. *Astr. Astrophys.*, **59**, 261.
- Davies, R. D., 1974. *The Formation and Dynamics of Galaxies, IAU Symp No. 58*, p. 119, ed. Shakeshaft, J. R., D. Reidel, Dordrecht, Holland.
- Dieter, N. H., 1962. *Astr. J.*, **67**, 313.
- Emerson, D. T., 1976. *Mon. Not. R. astr. Soc.*, **176**, 321.
- Heiles, C. R. & Habing, H. J., 1974. *Astr. Astrophys. Suppl.*, **14**, 1.
- Huchtmeier, W. K., 1975. *Astr. Astrophys.*, **45**, 259.
- Huchtmeier, W. K. & Witzel, A., 1979. *Astr. Astrophys.*, **74**, 138.
- Newton, K., 1978. *PhD thesis*, University of Cambridge.
- Newton, K. & Emerson, D. T., 1977. *Mon. Not. R. astr. Soc.*, **181**, 573.
- Nilson, P., 1973. *Uppsala General Catalogue of Galaxies*, Royal Society of Sciences, Uppsala, Sweden.
- Reakes, M. L. & Newton, K., 1978. *Mon. Not. R. astr. Soc.*, **185**, 277.
- Rogstad, D. H., Lockhart, I. A. & Wright, M. C. H., 1974. *Astrophys. J.*, **193**, 309.
- Rogstad, D. H., Shostak, G. S. & Rots, A. H., 1973. *Astr. Astrophys.*, **22**, 111.
- Rots, A. H., 1979. *Astr. Astrophys.*, in press.
- Sancisi, R., 1976. *Astr. Astrophys.*, **53**, 159.
- Tubbs, A. D. & Sanders, R. H., 1979. *Astrophys. J.*, **230**, 736.
- van der Kruit, P. C. & Allen, R. J., 1978. *A. Rev. Astr. Astrophys.*, **16**, 103.
- Warner, P. J., Wright, M. C. H. & Baldwin, J. E., 1973. *Mon. Not. R. astr. Soc.*, **163**, 163.
- Winter, A. J. B., 1975a. *Mon. Not. R. astr. Soc.*, **172**, 1.
- Winter, A. J. B., 1975b. *PhD thesis*, University of Cambridge.